Optical and Structural Properties of $Hg_{0.7}Cd_{0.3}Te$ Epitaxial Films

© D.A. Andryushchenko[1], M.S. Ruzhevich[1], A.M. Smirnov[1], N.L. Bazhenov[2], K.D. Mynbaev[2,¶], V.G. Remesnik[3]

[1] ITMO University,
197101 St. Petersburg, Russia
[2] Ioffe Institute,
194021 St. Petersburg, Russia
[3] Rzhanov Institute of Semiconductor Physics, Siberian Branch, Russian Academy of Sciences,
630090 Novosibirsk, Russia
¶ E-mail: mynkad@mail.ioffe.ru

Received May 31, 2021
Revised June 6, 2021
Accepted June 6, 2021

The results of comparative studies of the optical and structural properties of $Hg_{0.7}Cd_{0.3}Te$ bulk crystals and epitaxial films grown by various methods are presented. The data of photoluminescence studies performed in the temperature range 4.2−300 K showed the similarity of the optical properties of different samples and indicated a significant disordering of the solid solution. According to X-ray diffraction data, however, the scale of the disordering was not directly related to the structural quality of the material. The prospects for using the material grown by various methods in optoelectronics applications are discussed.

Keywords: HgCdTe, defects, luminescence, X-ray diffraction.

DOI: 10.21883/SC.2022.13.53899.9689

1. Introduction

The $Hg_{1-x}Cd_xTe$ (MCT) solid solutions are one of the main materials for producing instruments and devices designed to operate in the infrared (IR) spectrum region. Cadmium and mercury tellurides form a continuous row of solid solutions, which can be a base for producing photoelectronic and optoelectronic instruments designed to operate within the range of wavelengths λ from 1 to 14 μm. Presently, there is a growing interest to MCT with a molar fraction of CdTe (chemical composition) $x \approx 0.3$ as a material for middle-wave ($\lambda = 2-6\,\mu$m) infrared range [1–3]. This spectral range includes the lines of absorption, which is caused by rotational and vibrational resonances of molecules of many gases and liquids, including hydrocarbons. It is important for applications of environmental monitoring, security systems, energy audit, medicine, agriculture, etc. [4].

The MCT has been widely used for manufacturing photodetectors [5], but it is potentially considered a material for manufacturing emitters [6–8]. It has been a traditional opinion that the main problems for creating the emitters with interband optical MCT transitions were complexity in producing a property-homogeneous material with a large area and a high rate of Auger-recombination [4]. The MCT technology development creates the prerequisites to overcome these limitations. Specifically, using the molecular-beam epitaxy (MBE) for MCT growth on the Si substrates already allows producing plates of the diameter up to 8 inches [9]. In turn, the high rates of the Auger recombination can be suppressed in the plates by applying quantum-size structures [10], so can in the bulk material by applying the localization effect of the excitons of the carries on the composition fluctuations [11].

Presently, the most widespread MCT synthesis methods include MBE, the metal-organic vapor phase epitaxy (MOVPE) and the liquid-phase epitaxy (LPE). The material grown by each method has a typical defect structure and it can substantially affect parameters of devices being manufactured. The present paper provides results of the comparative studies of the optical and structural properties of the epitaxial MCT layers with $x \approx 0.3$ grown by various methods. It aims at analyzing prospects of application of these materials in various instrument structures.

2. Experimental procedure

The MBE-synthesized layers were produced on the GaAs(013) and Si(013) substrates with the ZnTe and CdTe buffer layers in Rzhanov Institute of Semiconductor Physics (Russia) by a procedure described in the paper [12]. The LPE-produced layers were grown in a grown system from tellurium-enriched melts on the Cd(Zn)Te(111) substrates in accordance with the procedure discussed in the paper [13]. After the growth, the samples were annealed in the Hg saturated vapor at 230°C during 48 h. For comparison, the samples of the bulk crystals were also studied, and the crystals were grown in JSC „Chistye Metally“ (Ukraine) by a modified method of vertically directed crystallization (VDC) with make-up out of the solid phase. The studies also involved the MOVPE-produced layers and some properties thereof have been previously reported in the paper [14]. They have been grown on the GaAs(110) semi-insulating substrates with the Cd(Zn)Te

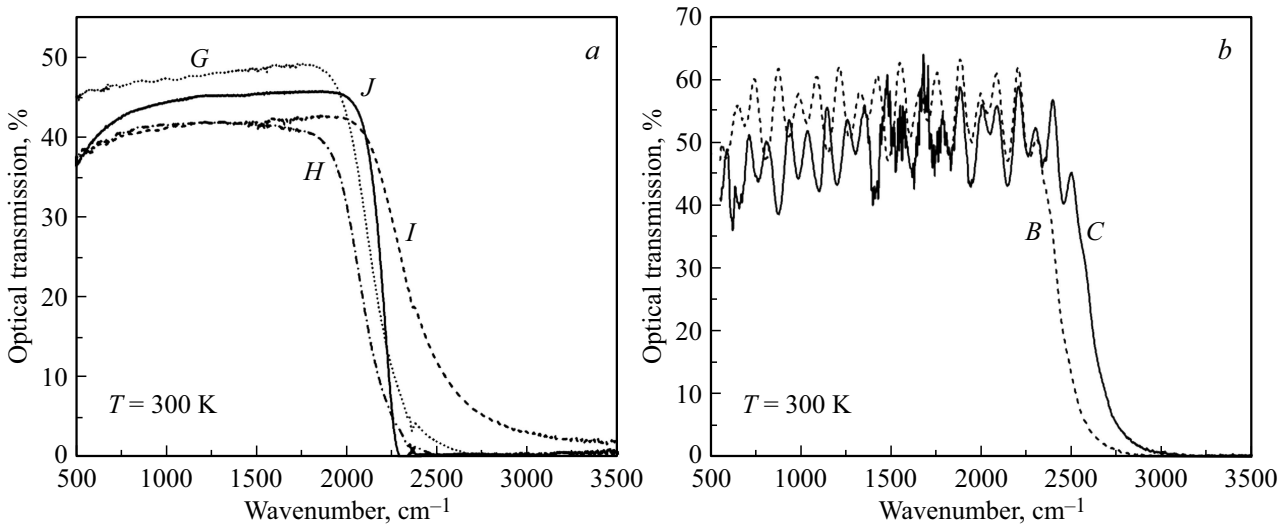

Figure 1. Spectra of optical transmission of the samples G, H, I and J (a), B and C (b).

Parameters of studied samples

Sample	Growth method	Substrate	x	Thickness of the film, μm
A	MBE	GaAs	0.30	5.0
B	MBE	GaAs	0.30	8.2
C	MBE	Si	0.32	8.1
D	MBE	Si	0.32	8.1
E	MOVPE	GaAs	0.32	10.0
F	MOVPE	GaAs	0.32	9.2
G	LPE	CdTe	0.32	16
H	LPE	CdZnTe	0.29	20
I	LPE	CdTe	0.30	12
J	VDC	–	0.30	–

buffer layer in the VIGO System S.A. company (Poland) as per a technology similar to that described in the paper [3]. The synthesis of these structures was completed by applying a thin CdTe layer, thereby forming a variable-gap surface MCT layer of the thickness to 0.5 μm during cooling. The parameters of the studied samples are given in the table. The chemical composition x and the thickness of the MBE-grown samples were evaluated by applying ellipsometric measurements *in situ* [12] and the studied of optical transmission (OP). For the LPE- and MOVPE-grown layers and for the samples of the bulk crystals, these parameters have been evaluated by the OP spectra and data of the optical microscopy.

The OP spectra were recorded at the temperature $T = 300$ K using the InfraLum-801 and FSM2203 Fourier spectrometers. The photoluminescence (PL) spectra were recorded within the temperature range 4.2–300 K using the mboxMDR-23 lattice monochromator. The PL signal was excited with a semiconductor laser of the wavelength of 1.03 μm and recorded with the InSb or HgCdTe photodetector. The structural studies were carried out by the DRON-8 X-ray gap-configured diffractometer with a thin-focus X-ray tube with a copper anode and scintillation detector NaI (Tl).

3. Results and discussion

Fig. 1 shows the OP spectra of the number of the studied samples. As it is clear, they are characterized by quite sharp transmission edges; the sharpest OP edge was typical for the sample of the bulk crystal (Fig. 1, a, the sample J), while the slope of the OP curves within the interband absorption was close for all the epitaxial layers. A position of the MBE edge for MBE-grown layers (Fig. 1, b) has corresponded to chemical composition values determined as per ellipsometric data. These samples were characterized by typical interference bands at small wave numbers.

Fig. 2 shows normalized spectra of the PL samples A, B, C and D (Fig. 2, a), and E (of the paper [14]), H and J (Fig. 2, b), as recorded at 85 K. The full width at the half-height (the half-width) of the spectra recorded at this temperature was 14.8 meV for the sample A, 15.0 meV for the samples B and C, 12.6 meV for the sample D, 17.2 meV for the sample I, 15.7 meV for the samples J and K and 19.4 meV for the sample H. The spectra of the MOVPE-grown samples E and F were substantially wider, and their half-widths at 85 K were 31 and 28 meV, respectively. It could be caused by the fact that in this case the solid solution was formed by mutual diffusion of components of the CdTe and HgTe compounds, which were applied during the epitaxy in thin layers layer-by-layer [3], which could contribute to some composition heterogeneity of the epitaxial layer along it thickness. At $T = 4.2$ K, the half-width of the PL spectra was 7.3 meV for the C sample, 6.5 meV for the D sample and 16.2 meV for the E sample.

Fig. 3 shows examples of the temperature dependences of the maximum positions of the PL bands $E_{PL}(T)$ for some samples (symbols), and the dependence of the

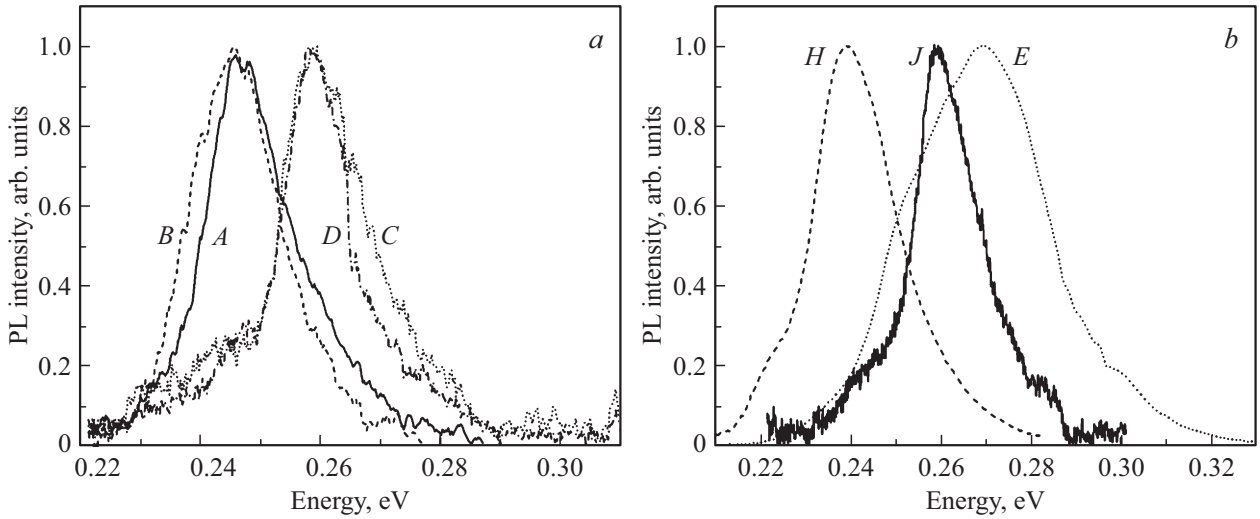

Figure 2. Photoluminescence spectra of the A, B, C and D (a), E, H and J (b) samples recorded at the temperature of 85 K. Noise level differences on the spectra are caused by differences in the PL signal intensity and in spectrum recording conditions.

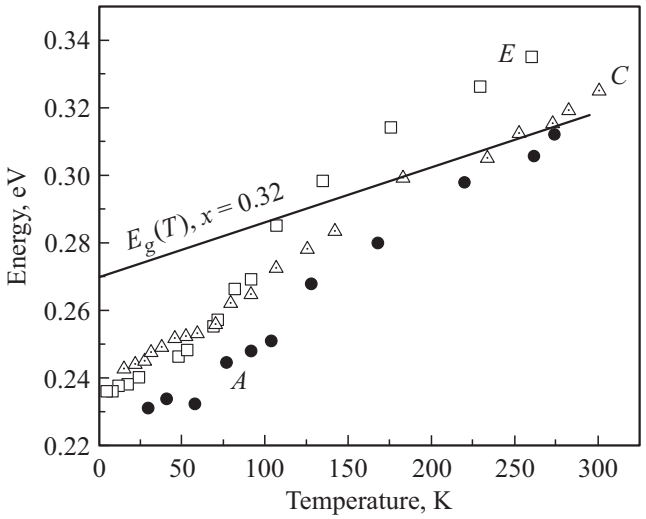

Figure 3. Temperature dependences of the maximum positions of the PL bands for the A, C and E samples (symbols) and the dependence $E_g(T)$ for MCT with $x = 0.32$ as per the data of the paper [15] (the solid curve).

band gap $E_g(T)$, calculated for MCT with $x = 0.32$ in accordance with an empirical relationship $E_g(x, T)$ of the paper [15] (the solid curve). As it is clear, the experimental dependences have a close slope and it differs from the slope of the calculated dependence $E_g(T)$. This difference was observed for all the studied samples and correlated to the fact that the MCT optical transitions at low temperatures are caused by recombination of the excitons which were localized at the composition fluctuations [16–19]; at the same time, it is known that for the LPE-grown MCT layers the difference between E_{PL} and E_g at the low temperatures is substantially lower than for the MBE-produced layers [20]. The $E_{PL}(T)$ behavior for the E sample could be correlated to an available variable-gap surface layer or to the above-said composition heterogeneity and requires further studies. For the E and F samples, the photoconductivity spectra were recorded at $T = 85$ K (for the E sample the spectrum is given in the paper [14]). The position of the half-drop of the long-wave photoconductivity interface for both the samples corresponded to the energy of ~ 0.28 eV, which corresponded to a claimed composition of the film as per the used dependence $E_g(x, T)$.

Fig. 4, a shows the diffraction pattern of the sample of the MCT bulk crystal (the J sample). It has a single peak at $2\theta \approx 23.79°$ corresponding to the crystal-lattice plane HgCdTe(111). A low intensity of this peak indicates a relatively low crystal perfection of the sample; it is confirmed by no reflection from the planes (222) and (444), which we observe in similar conditions for the MCT bulk crystal with $x \approx 0.7$ [21]. The X-ray diffraction (XD) swinging curve of this sample (not shown) indicates multiple single units with the (111) orientation, which are disoriented to each other; its half-width was 0.9° (for the single crystal with $x \approx 0.7$, as considered in the paper [21], it was 0.4°).

The diffraction patterns of the LPE-grown layers had five peaks. Fig. 4, b shows the diffraction pattern for the H sample. In contrast to the others, the first peak (the peak I) at $2\theta \approx 21.52°$ was not separated into $K_{\alpha 1}$ and $K_{\alpha 2}$; it is possible, in the same way as with the crystal with $x \approx 0.7$ [21], its presence was of an accompanying character and caused by oxidation of the sample surface. The peak II at $2\theta \approx 23.84°$ corresponded to the HgCdTe (111) plane. There were also long-range orders of reflections from the (111) planes: the (222) planes (the peak III at $2\theta \approx 48.77°$) and (444) (the peak V at $2\theta \approx 111.25°$), but however the intensity of the reflected beam from the (222) plane was lower than from the (444) plane. Furthermore, the diffraction pattern also had reflection from the (511)

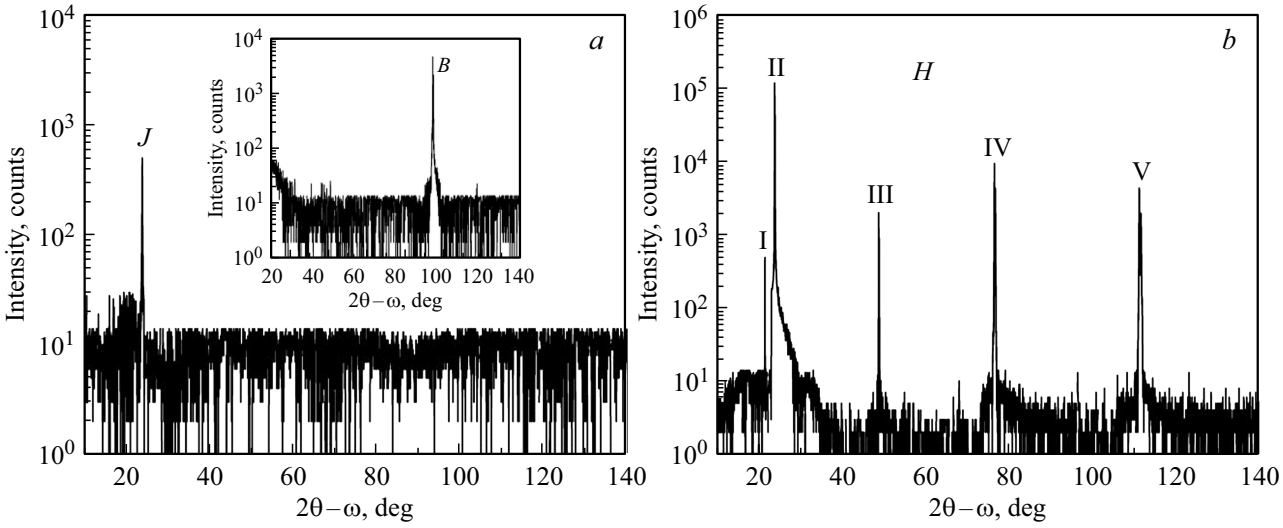

Figure 4. Diffraction patterns of the samples J (the B sample of the insert) (a) and H (b).

plane (the peak IV at $2\theta \approx 76.51^\circ$). Generally, both the LPE-grown films had a polycrystalline structure with the units with the orientation [111] and [511] and high crystal perfection of separate units. The half-width values of the XD swinging curves for these films were within the range $100-150''$.

The diffraction pattern of the B and C samples (the insert of Fig. 4, a shows the diffraction pattern for the B sample) were similar to those for the films with the compositions $x \approx 0.7$ and $x \approx 0.4$, discussed in the papers [21,22]. There was domination of the peak at $2\theta \approx 97.8^\circ$, which is typical for the MBE MCT diffraction patterns [22]. The half-width of this peak for the B sample was $3236''$ ($2\theta \approx 97.81^\circ$), so was for the C sample— $1038''$ ($2\theta \approx 97.76^\circ$). The set of the peaks at $25-36^\circ$ was most likely correlated to superposition of multiple peaks from separate layers making up a heteroepitaxial structure [21].

Thus, as per XD data, the highest crystal quality among the studied samples was for the LPE-grown layers. The sharp OP edge and the relatively small half-width of the PL peak at 85 K, which are typical for the studied samples of the MCT bulk crystals, were not correlated to the relatively low crystal perfection (as per the XD results). Despite ambiguous results of the XD studies, the MCT MBE-grown layers with $x \approx 0.3$ showed low values of the half-widths of the low temperature PL spectra and no optical transition with involvement of the states correlated to uncontrollable impurities, which are typical for similar layers of bigger compositions [19]. Among all the studied samples, only the MBE- and MOVPE-grown layers exhibited the PL signal at $T > 150$ K. It can be explained by scaling „technological" fluctuations in addition to stochastic fluctuations therein; these fluctuations contribute to stronger localization of the excitons [11,19]. Thus, it is obviously this material, which is the most promising for manufacturing the middle-wave IR-range emitters based on MCT.

4. Conclusion

The paper includes the studies of the optical and structural properties of the bulk crystals and the epitaxial films $Hg_{0.7}Cd_{0.3}Te$, which are grown by various methods. The form and the half-width (from ~ 13 to ~ 20 meV at 85 K) of the photoluminescence spectra of all the samples were similar. The temperature dependences of the maximum position of the luminescence peak indicated disordering of the solid solution. It can be noted that as per the data of X-ray diffraction the scale of this disordering was not directly correlated to a structural quality of the material. That is why further studies are required its nature and impact on non-optical properties (transport, etc.).

Acknowledgments

The authors would like to thank N.N. Mikhailov, M.V. Yakushev and V.S. Varavin for providing the MBE-grown samples, and M.A. Remennoy for help in implementing the measurements of optical transmission.

Conflict of interest

The authors declare that they have no conflict of interest.

References

[1] F.Y. Yue, S.Y. Ma, J. Hong, P.X. Yang, C.B. Jing, Y. Chen, J.H. Chu. Chin. Phys. B, **28**, 017104 (2019).
[2] X.F. Qiu, S.X. Zhang, J. Zhang, Y.C. Zhu, C. Dou, S.C. Han, Y. Wu, P.P. Chen. Crystals, **11**, 296 (2021).
[3] M. Kopytko, J. Sobieski, W. Gawron, A. Kebłowski, J. Piotrowski. Semicond. Sci. Technol., **36**, 055003 (2021).
[4] D. Jung, S. Bank, M.L. Lee, D. Wasserman. J. Opt., **19**, 123001 (2017).

[5] W. Lei, J. Antoszewski, L. Faraone. Appl. Phys. Rev., **2**, 041303 (2015).
[6] C.R. Tonheim, A.S. Sudbø, E. Selvig, R. Haakenaasen. IEEE Photon. Technol. Lett., **23**, 36 (2011).
[7] J.P. Zanatta, F. Noël, P. Ballet, N. Hdadach, A. Million, G. Destefanis, E. Mottin, C. Kopp, E. Picard, E. Hadji. J. Electron. Mater., **32**, 602 (2003).
[8] E. Hadji, E. Picard, C. Roux, E. Molva, P. Ferret. Optics Lett., **25**, 725 (2000).
[9] M. Reddy, X. Jin, D.D. Lofgreen, J.A. Franklin, J.M. Peterson, T. Vang, N. Juanko, F. Torres, K. Doyle, A. Hampp, S.M. Johnson, J.W. Bangs. J. Electron. Mater., **48**, 6040 (2019).
[10] V.Ya. Aleshkin, V.V. Rumyantsev, K.E. Kudryavtsev, A.A. Dubinov, V.V. Utochkin, M.A. Fadeev, G. Alymov, N.N. Mikhailov, S.A. Dvoretsky, F. Teppe, V.I. Gavrilenko, S.V. Morozov. J. Appl. Phys., **129**, 133106 (2021).
[11] A.V. Shilyaev, K.D. Mynbaev, N.L. Bazhenov, A.A. Greshnov. ZhTF, **87**, 419 (2017) (in Russian).
[12] Y.G. Sidorov, V.S. Varavin, S.A. Dvorestkiy, N.N. Mikhailov, M.V. Yakushev, I.V. Sabinina. FTP, **35**, 1092 (2001) (in Russian).
[13] K.E. Mironov, V.K. Ogorodnikov, V.D. Rozumnyi, V.I. Ivanov-Omskii. Phys. Status Solidi A, **78**, 125 (1983).
[14] I.I. Izhnin, A.I. Izhnin, E.I. Fitsych, J. Piotrowski, K.D. Mynbaev. Izv. vuzov. Fizika, №. 9/2, 89 (2013) (in Russian).
[15] C.R. Becker, V. Latussek, A. Pfeuer-Jeschke, G. Landwehr, L.W. Molenkamp. Phys. Rev. B, **62**, 10353 (2000).
[16] R. Legros, R. Triboulet. J. Cryst. Growth, **72**, 264 (1985).
[17] P. Gille, K.H. Herrmann, N. Puhlmann, M. Schenk, J.W. Tomm, L. Werner. J. Cryst. Growth, **86**, 593 (1988).
[18] A. Lusson, F. Fuchs, Y. Marfaing. J. Cryst. Growth, **101**, 673 (1990).
[19] K.D. Mynbayev, N.L. Bazhenov, V.I. Ivanov-Omsky, N.N. Mikhailov, M.V. Yakushev, A.V. Sorochkin, V.G. Remesnik, S.A. Dvorestkiy, V.S. Varavin, Yu.G. Sidorov. FTP, **45**, 900 (2011) (in Russian).
[20] I.I. Izhnin, A.I. Izhnin, K.D. Mynbaev, N.L. Bazhenov, A.V. Shilyaev, N.N. Mikhailov, V.S. Varavin, S.A. Dvoretsky, O.I. Fitsych, A.V. Voitsekhovsky. Opto-Electron. Rev., **21**, 390 (2013).
[21] K.D. Mynbayev, N.L. Bazhenov, A.M. Smirnov, N.N. Mikhailov, V.G. Remesnik, M.V. Yakushev. FTP, **54**, 1302 (2020) (in Russian).
[22] D.A. Andryushchenko, I.N. Trapeznikova, N.L. Bazhenov, M.A. Yagovkina, K.D. Mynbaev, V.G. Remesnik, V.S. Varavin. J. Phys. Conf. Ser., **1400**, 066038 (2019).